

A Real-time Estimator of Electrical Parameters for Vector Controlled Induction Motor using a Reduced Order Extended Kalman Filter

Vicente Leite¹⁾, Rui Araújo²⁾, Diamantino Freitas³⁾

¹⁾ ESCOLA SUPERIOR DE TECNOLOGIA E DE GESTÃO DO INSTITUTO
POLITÉCNICO DE BRAGANÇA

Campus de Santa Apolónia, Apartado 134, 5301-857 Bragança
Bragança, Portugal

E-mail: avtl@ipb.pt

Phone n.º: 351-273-303158, fax n.º: 351-273-313051

^{2,3)} FACULDADE DE ENGENHARIA DA UNIVERSIDADE DO PORTO

Rua Dr. Roberto Frias s/n, 4200-465 Porto

Porto, Portugal

E-mail: ²⁾ raraujo@fe.up.pt, ³⁾ dfreitas@fe.up.pt

Phone n.º: ²⁾ 351-22-5081808, ³⁾ 351-22-5081837; fax n.º: ^{2,3)} 351-22-5081443

Keywords

Induction motors, estimation techniques, variable speed drives, adaptive control.

Abstract

This paper presents an application of the extended Kalman filter (EKF) to the simultaneous on-line estimation of the dq rotor flux components and all the electrical parameters of a vector controlled induction motor. A time-discrete reduced order model structure is deduced and presents a simple and reduced state equation and a scalar output equation. This approach, combined with the use of the rotor reference frame, offers advantages for real-time identification, compared with full order models, because it reduces the computational cost. The proposed new approach requires the measurement of motor speed, stator voltages and currents signals. Simulation and experimental studies presented in this paper highlight the improvements produced by this new approach based on the extended Kalman filter and a new discretization technique, under real operation conditions.

Introduction

Last decades were very productive for control of the induction motor. We have witnessed the development of increasingly sophisticated control methods, from simple scalar methods to vector control, and, more recently, to sliding mode control strategies. Although these methods are used currently in industrial applications, many of them require the knowledge of the motor model parameters, because a mismatch in these ones is prone to create unacceptable control errors. In fact, the electric parameters characterizing the induction motor model can vary significantly during the normal operation of the motor. This is caused by phenomena such as stator and rotor heating, magnetic saturation and skin effect. Thus, uncertainty and parameter variations can deteriorate the achieved control. The effects of parameter sensitivity on the performance in vector control schemes and the possibility of identification of the changes in motor parameters while the drive is in its normal operation have been given in [1]. Therefore, it is necessary to estimate and track the parameter values in real-time operation. Many parameter identification algorithms based on the least squares method family, observer theory, and so forth, have been proposed in the relevant scientific literature. Among them, the Kalman filter based algorithms have been demonstrated to be the best for processing noisy discrete measurements while obtaining accurate estimates [2-9]. The extended Kalman filter is a recursive, optimal, real-time data processing algorithm for nonlinear systems for both state and parameters estimation [10] of a dynamic system in a noisy environment. When a PWM inverter is employed to feed the induction motor the fundamental components are considered as deterministic inputs or outputs depending on the model structure, and the wideband harmonics components are

included in the noise vectors of the state-space model structure [11]. The noise vectors are assumed to be white, zero-mean Gaussian, and independent.

A large amount of works have been developed on this subject. Many are treating single parameter identification, namely rotor time constant or rotor resistance, with rotor flux estimation for indirect vector control purposes. Two approaches are used: full order models [2-5] or reduced order models motivated by less computational effort [5-9]. In [3] the rotor reference frame is used and the others work in the stator reference frame. Two works [3, 8] are related to the identification of all the parameters. In this paper the authors present a new approach for two rotor flux components and all the physical parameters of the three-phase squirrel cage induction motor with an algorithm which is based on a reduced order model of the induction motor in rotor reference frame, using the extended Kalman Filter and a particular discretization technique of the continuous-time model.

Induction motor model

The well-known established model of the induction motor in the rotor reference frame is represented, like in [11], by its stator and rotor space phasors voltage equations and stator and rotor flux equations expressed in terms of stator and rotor currents space phasors. Considering a squirrel-cage induction motor and eliminating stator flux and rotor currents space phasors with some algebraic manipulation, the following equations can be obtained:

$$\bar{i}_s^r(t) = -(a + j\omega)\bar{i}_s^r(t) + L_s'^{-1}(\tau_r^{-1} - j\omega)\bar{\psi}_r^r(t) + L_s'^{-1}\bar{u}_s^r(t) \quad (1)$$

$$\bar{\psi}_r^r(t) = L_M \tau_r^{-1} \bar{i}_s^r(t) - \tau_r^{-1} \bar{\psi}_r^r(t) \quad (2)$$

$$\text{Where } a = \frac{R_s}{L_s'} + \frac{L_M}{L_s' \tau_r}, \quad \bar{\psi}_r^g(t) = \frac{L_m}{L_r} \bar{\phi}_r^g, \quad \tau_r = \frac{L_r}{R_r}, \quad L_s' = L_s - \frac{L_m^2}{L_r}, \quad \text{and } L_M = \frac{L_m^2}{L_r} \quad (3)$$

For computational convenience the equations above are usually converted into state-space-based form of 4th order with only real quantities as follows.

$$\begin{bmatrix} \dot{i}_{sd}^r \\ \dot{i}_{sq}^r \\ \dot{\psi}_{rd}^r \\ \dot{\psi}_{rq}^r \end{bmatrix} = \begin{bmatrix} -a & \omega & L_s'^{-1} \tau_r^{-1} & \omega L_s'^{-1} \\ -\omega & -a & -\omega L_s'^{-1} & L_s'^{-1} \tau_r^{-1} \\ L_M \tau_r^{-1} & 0 & -\tau_r^{-1} & 0 \\ 0 & L_M \tau_r^{-1} & 0 & -\tau_r^{-1} \end{bmatrix} \begin{bmatrix} i_{sd}^r \\ i_{sq}^r \\ \psi_{rd}^r \\ \psi_{rq}^r \end{bmatrix} + \begin{bmatrix} L_s'^{-1} & 0 \\ 0 & L_s'^{-1} \\ 0 & 0 \\ 0 & 0 \end{bmatrix} \begin{bmatrix} u_{sd}^r \\ u_{sq}^r \end{bmatrix} \quad (4)$$

The time-domain state-space model is formed by the state equation above and an output equation:

$$\frac{dx(t)}{dt} = Ax(t) + Bu(t) \quad \text{and} \quad y(t) = Cx(t) \quad (5)$$

$$\text{Where } x(t) = \begin{bmatrix} i_{sd}^r & i_{sq}^r & \psi_{rd}^r & \psi_{rq}^r \end{bmatrix}^T \quad \text{and} \quad y(t) = \begin{bmatrix} 1 & 0 & 0 & 0 \\ 0 & 1 & 0 & 0 \end{bmatrix} \begin{bmatrix} i_{sd}^r \\ i_{sq}^r \end{bmatrix} \quad (6)$$

A time-discrete state-space model can next be obtained by assuming that the series expansion of the matrix exponential function e^{AT_s} is performed and only the first terms are considered [12]. Since for a small sampling interval, T_s , matrices A and B can be considered to be constant during the sample period, only the linear terms will be considered:

$$A_d(k) = I + AT_s + \frac{A^2 T_s^2}{2!} + \frac{A^3 T_s^3}{3!} + \dots \quad \text{and} \quad B_d(k) = \left(T_s + \frac{AT_s^2}{2!} + \frac{A^2 T_s^3}{3!} + \dots \right) B \quad (7)$$

We will adopt a different strategy to the model structure and model discretization by selecting the reduced order model obtained by considering equation (2) as a state equation, since stator currents are measured, and by forming the output equation from equation (1). Considering separate real and imaginary parts of complex equation (2) the state equation becomes:

$$\begin{bmatrix} \dot{\psi}_{rd}^r \\ \dot{\psi}_{rq}^r \end{bmatrix} = \begin{bmatrix} -\tau_r^{-1} & 0 \\ 0 & -\tau_r^{-1} \end{bmatrix} \begin{bmatrix} \psi_{rd}^r \\ \psi_{rq}^r \end{bmatrix} + \begin{bmatrix} L_M \tau_r^{-1} & 0 \\ 0 & L_M \tau_r^{-1} \end{bmatrix} \begin{bmatrix} i_{sd}^r \\ i_{sq}^r \end{bmatrix} \quad (8)$$

It is important to notice here that both equations that result from real and imaginary parts of equation (1) have the same structure with the same states (parameters) and the same signals (voltages and currents components), but shifted in time. Therefore, they contain the same information for identification purposes. So we will use here only one of them, for instance, the first one. The output equation becomes, after rewriting those terms:

$$u_{sd}^r(t) = -\tau_r^{-1} \psi_{rd}^r(t) - \omega(t) \psi_{rq}^r(t) + a i_{sd}^r(t) + L_s' (i_{sd}^r - \omega(t) i_{sq}^r(t)) \quad (9)$$

Equations (8) and (9) form a 2nd order state-space model structure instead of a 4th order one, as usually with (4) and (6). It is worth noting that this is an important and new simplification transforms the initial model into a single and therefore scalar output model structure. Since the state equation (8) has a reduced order, half of its matrix elements are zero and the output equation is treated separately, it becomes very simple and not fastidious to obtain a 2nd order approximation. For the continuous state equation (8) we can easily obtain, by using (7), the 1st order time-discrete state equation as follows, corresponding to the Euler's formula.

$$\begin{bmatrix} \psi_{rd}^r(k+1) \\ \psi_{rq}^r(k+1) \end{bmatrix} = \begin{bmatrix} 1 - T_s \tau_r^{-1} & 0 \\ 0 & 1 - T_s \tau_r^{-1} \end{bmatrix} \begin{bmatrix} \psi_{rd}^r(k) \\ \psi_{rq}^r(k) \end{bmatrix} + \begin{bmatrix} T_s L_M \tau_r^{-1} & 0 \\ 0 & T_s L_M \tau_r^{-1} \end{bmatrix} \begin{bmatrix} i_{sd}^r(k) \\ i_{sq}^r(k) \end{bmatrix} \quad (10)$$

The choice of estimation of rotor flux components instead of rotor current components is advisable because in light load conditions the rotor currents are very small and bad convergence and estimation results can arise as referred in [5]. Furthermore, the magnitudes of the rotor flux components are much more uniform in different load conditions.

For the first derivative of the d component stator current in output equation (9), instead of Euler's formula, a better recursive approximation to the first derivative will be used and the output equation becomes:

$$\begin{aligned} u_{sd}^r(k) = & -\tau_r^{-1} \psi_{rd}^r(k) - \omega(k) \psi_{rq}^r(k) + a i_{sd}^r(k) + \\ & + L_s' \left(\frac{1}{2T_s} (3i_{sd}^r(k) - 4i_{sd}^r(k-1) + i_{sd}^r(k-2)) - \omega(k) i_{sq}^r(k) \right) \end{aligned} \quad (11)$$

Extended Kalman Filter (EKF)

The discrete-time EKF is a recursive state and parameter estimator suitable for use with multi-input, multi-output nonlinear time-varying stochastic plant models. By choosing the values in the covariance matrices, the EKF can be tuned to the noise characteristics of the measured outputs and the initial uncertainties in the estimated states and parameters. The process noise covariance matrix allows the use of models, which have true disturbances in their states and parameters, or models, which are not quite correct in their structure. The mechanisms that cause the state and parameter changes does not need to be known. In this paper, a particular initialization of the process covariance matrix is presented to improve the filter dynamics during start-up. The EKF is used, here, to estimate the rotor flux dq components and all physical parameters of the induction motor, modeled as above, this being usually classified as a reduced order model, with a different output equation in this case. The EKF can be used for both state and parameter estimation by treating the physical induction motor parameters as additional states and forming an augmented state vector. As a result, even if the original state-space model is linear, the augmented one is nonlinear because of inter-multiplication of states. The EKF deals directly with this nonlinear augmented model. To use the EKF with nonlinear plant models, the model structure must be linearized around an operating point to produce a linear perturbation model. Here the application of the EKF to the simultaneous estimation of rotor flux together with induction motor parameters produces a sixth-order extended state-space model with the following state vector:

$$x_e(k) = [x_{e1}(k) \quad \cdots \quad x_{e6}(k)]^T = [x_1(k) \quad x_2(k) \quad \theta_1(k) \quad \cdots \quad \theta_4(k)]^T =$$

$$= [\psi_{rd}^r(k) \quad \psi_{rq}^r(k) \quad \tau_r^{-1}(k) \quad L_s'(k) \quad L_M(k) \quad R_s(k)]^T \quad (12)$$

where the subscript e denotes the extended or augmented state vector. For the estimation of the parameters, four extra equations are obtained by assuming a random walk to their adaptation as referred in the literature [10]:

$$\theta_j(k+1) = \theta_j(k) + r_{\theta_j}(k) \quad (13)$$

Consider the stochastic time-discrete nonlinear state-space model [10]:

$$x_e(k+1) = f(x(k), u(k), \theta(k)) + r_{se}(k) \quad (14)$$

$$y(k) = h(x(k), \theta(k)) + r_m(k) \quad (15)$$

$$x_e(0) = x_e(x(0), \theta(0)) \quad (16)$$

It is usually assumed that the process noise $r_{se}(k)$ and measurement noise $r_m(k)$ are white, zero-mean Gaussian and independent sequences.

The associated EKF algorithm is given as follows:

1. Determination of the initial conditions:

$$\begin{cases} E\{x(0)\} = \hat{x}_e(0) \\ E\{(x_e(0) - \hat{x}_e(0))(x_e(0) - \hat{x}_e(0))^T\} = P(0) \end{cases}$$

$$2. \hat{x}_e(k+1|k) = \begin{bmatrix} f(\hat{x}(k|k), u(k), \hat{\theta}(k|k)) \\ \theta(k) \end{bmatrix} + \begin{bmatrix} r_s(k) \\ r_{\theta}(k) \end{bmatrix} = f_e(\hat{x}_e(k|k), u(k)) + r_{se}(k)$$

$$3. F(k) = \left. \frac{\partial f_e(x_e(k), u(k))}{\partial x_e^T(k)} \right|_{x_e(k)=\hat{x}_e(k|k)} = \left[\begin{array}{cc} \frac{\partial f_e(x(k), u(k), \theta(k))}{\partial x^T(k)} & \frac{\partial f_e(x(k), u(k), \theta(k))}{\partial \theta^T(k)} \\ 0 & I \end{array} \right] \Bigg|_{\hat{x}_e(k|k)}$$

$$4. \hat{P}(k+1|k) = F(k)\hat{P}(k|k)F^T(k) + R_s$$

$$5. H(k) = \left. \frac{\partial h_e(x_e(k))}{\partial x_e^T(k)} \right|_{\hat{x}_e(k+1|k)} = \left[\begin{array}{cc} \frac{\partial h(x(k), \theta(k))}{\partial x^T(k)} & \frac{\partial h(x(k), \theta(k))}{\partial \theta^T(k)} \end{array} \right] \Bigg|_{\hat{x}_e(k+1|k)}$$

$$6. K(k+1) = \hat{P}(k+1|k)H^T(k)[H(k)\hat{P}(k+1|k)H^T(k) + R_m]^{-1}$$

$$7. \hat{y}(k+1) = h(\hat{x}_e(k+1|k), k)$$

$$8. \hat{x}_e(k+1|k+1) = \hat{x}_e(k+1|k) + K(k+1)[y(k+1) - \hat{y}(k+1)]$$

$$9. \hat{P}(k+1|k+1) = [I - K(k+1)H(k)]\hat{P}(k+1|k)$$

10. Go to step 2

Considering the linear terms in (7) and from equation (10) the functions f_e to the reduced order model of the induction motor presented here are as follows:

$$x_{e1}(k+1) = f_{e1}(x_e(k), u(k), k) = (1 - T_s x_{e3}(k))x_{e1}(k) + T_s x_{e3}(k)x_{e5}(k)i_{sd}(k) + r_{se1}(k) \quad (17)$$

$$x_{e2}(k+1) = f_{e2}(x_e(k), u(k), k) = (1 - T_s x_{e3}(k))x_{e2}(k) + T_s x_{e3}(k)x_{e5}(k)i_{sq}(k) + r_{se2}(k) \quad (18)$$

$$x_{ej}(k+1) = f_{ej}(x_e(k), u(k), k) = x_{ej}(k) + r_{sej}(k), \quad j = 1, 2, 3, 4 \quad (19)$$

The output equation is:

$$y(k) = h(x_e(k), k) = -x_{e3}(k)x_{e1}(k) - \omega(k)x_{e2}(k) + (x_{e6}(k) + x_{e3}(k)x_{e5}(k))i_{sd}(k) + \left(\frac{1}{2T_s} (3i_{sd}^r(k) - 4i_{sd}^r(k-1) + i_{sd}^r(k-2)) - \omega(k)i_{sq}(k) \right) x_{e4}(k) + r_m(k) \quad (20)$$

Simulation Results

The above-proposed algorithm has been developed in the *Matlab* with *Simulink* environment and tested under a vector control scheme. The rotor-referred stator voltages, stator currents and angular speed are sampled at 2,5kHz. Elliptic low-pass pre-filters of fifth order with a 500Hz cutoff frequency were used. These simulation conditions were chosen to be the same as the experimental ones in previous work [13] and will be used in experimental results presented in the next section. A trial of simulations shows that several important and difficult aspects arise when trying to estimate simultaneously rotor flux and all induction motor parameters with a reduced order model. On the one hand the noise covariance matrices must be correctly set, the state-vector and error covariance matrix initialized, the state vector properly scaled and, on the other hand, the signals must be persistent and the model structure identifiable. All induction motor state-space model structures with state vector including fluxes or currents and direct or modified physical parameters of the machine, will have significantly different magnitudes of state variables. When the model structure contains parameters with different orders of magnitude, it is mandatory to scale the variables so that they all get roughly the same magnitude. Oppositely, if we do not scale the state vector states (in this case), significant estimation errors occur for small sized variables and some numerical problems arise. To overcome this problem, the following scaled state vector has been selected:

$$x = [\psi_{rd} \quad \psi_{rq} \quad 0.2 \times \tau_r^{-1} \quad 50 \times L_s' \quad 5 \times L_M \quad 0.5 \times R_s]^T \quad (21)$$

As a result, the diagonal initial values of the state covariance matrix and the diagonal elements of process and measurement noise covariance matrices will approximately have the same values and the same conclusion is applicable to the initial values of the state variables. The EKF has been started with the following initial conditions:

$$\begin{cases} x(0) = [0.1 \quad 0.1 \quad 0.1 \quad 0.1 \quad 0.1 \quad 0.1]^T \\ P(0) = \text{diag}[1e-5 \quad 1e-5 \quad 1e-5 \quad 1e-5 \quad 1e-5 \quad 1e-5] \\ R_m = 0.01 \end{cases} \quad (22)$$

It should be noticed that the measurement matrix R_m is no more a matrix but a single value because the system output becomes a scalar equation instead of a matrix one. As to the initialization of the process noise system matrix, some improvements were also introduced. To get a good trade off between starting period of parameters convergence and tracking of time varying parameters, the filter dynamics (and in the sequel the noise covariance matrices R_m and R_s) should be properly tuned during these two phases. It is known that the larger the i th diagonal entry of R_s is, the more quickly the filter will modify the estimate of the i th component (flux or parameter) of the state vector in the light of the measurements. In other words, the larger the correction gain is, for any given R_m , the jitterier the behaviour of the filter will be, and more drastically the state estimate will be modified to take new measurements into account. This behaviour expresses a lack of confidence in the predicted state estimate. Conversely, for any given R_s , the larger the covariance of measurement noise R_m is, the smaller the correction gain will be and the less the new measurements will be taken into account to update the state estimate. This expresses a lack of confidence in the new measurements. So, it is possible to get a reasonably compromise between the state update dynamics when starting the algorithm in which the state variables are far away of their real values, and the dynamics for tracking the time variant states after that transient period. In this work, a simple approach was used to do this, by using an exponential function to each i th diagonal element corresponding to parameters, as follows:

$$R_s(k) = \text{diag}[1e-8 \quad 1e-8 \quad g_1(k) \quad g_2(k) \quad g_3(k) \quad g_4(k)] \quad (23)$$

$$\text{with } g_{1,2,3}(k) = 1e-8 \times (\exp(-0.8kT_s) + 0.01) \text{ and } g_4(k) = 1e-7 \times (\exp(-0.8kT_s) + 0.01) \quad (24)$$

The identification tests consist of a start-up transient with a load torque of 12Nm and a start-up transient followed by a serial of changes in speed reference between 500 and 1500rpm. This last test was also investigated with no load torque. Simulation and experimental identification tests with the start-up transient show that slightly different estimated values of stator resistance R_s , can occur when different values of the respective diagonal element of the state covariance matrix are selected what does not happen with the other parameters. This requires a difficult and careful initial tuning of the EKF. This difficulty results from the input signals of the model being not persistent enough to stimulate the stator parameters, mainly R_s , in the steady state operation after the start-up transient. Introducing some dynamics to the induction motor like a square speed reference as presented in the next figures, such a problem does not appear.

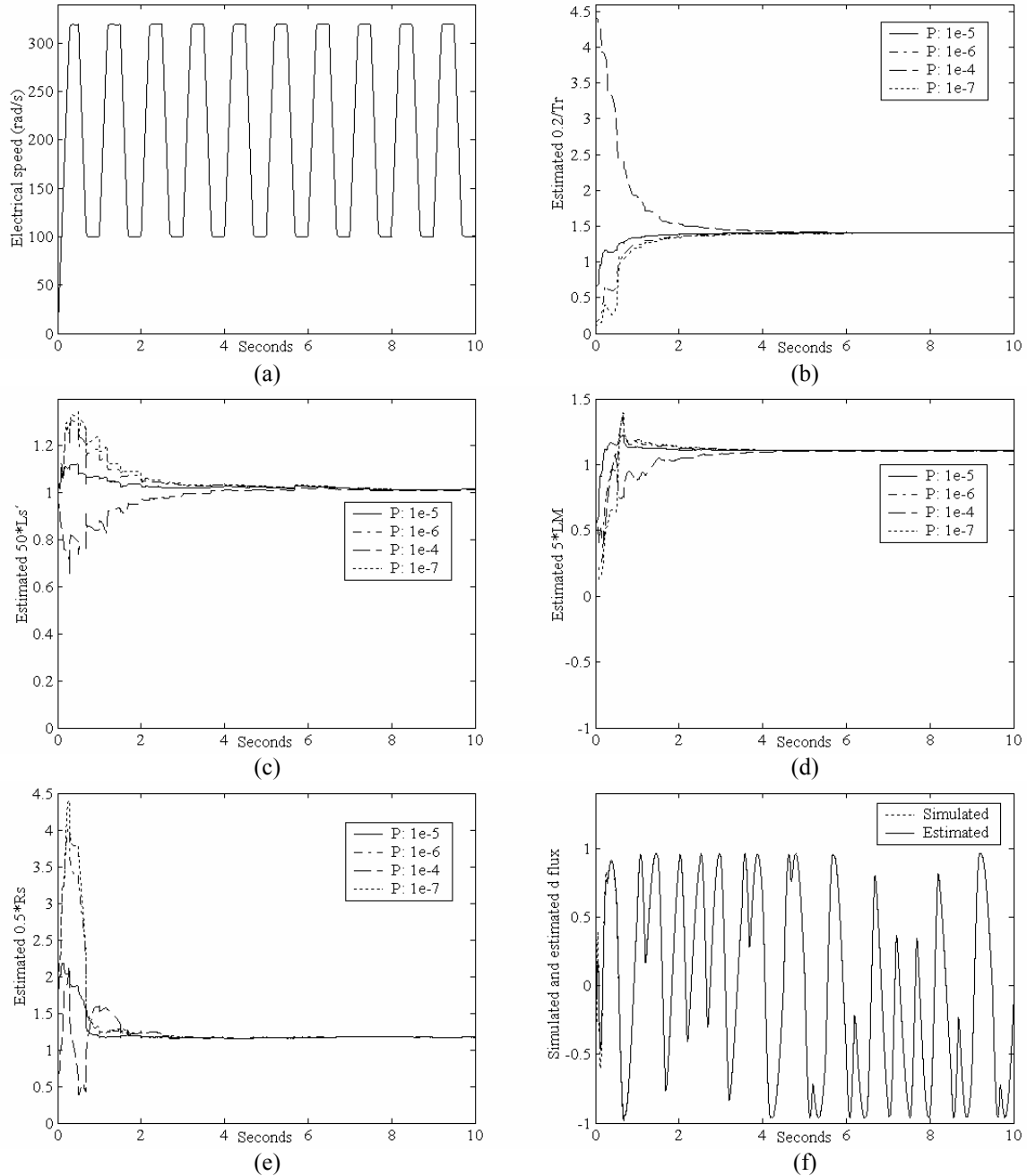


Fig. 1: Robustness test of estimated states convergence with respect to initial state covariance matrix ($P=\text{diag. element of } P(0)$), with a load torque of 12Nm. (a) Simulated electrical speed, (b) estimated $0.2 \times \tau_r$, (c) estimated $50 \times L_s'$, (d) estimated $5 \times L_M$, (e) estimated $0.5 \times R_s$, (f) simulated and estimated d flux component.

Figure 1 shows the robustness of estimated flux and parameters convergence with respect to initial state covariance matrix, with a load torque of 12Nm. As we can see from plots 1 (b) to (e) the implemented algorithm has a good convergence with respect to different initial state covariance matrix diagonal elements. Figure 1 (a) shows the electrical speed generated by the vector control scheme of the induction motor implemented in *Simulink*. Figure 1 (f) shows simulated and estimated flux where only d component is presented. Figure 2 shows the robustness of estimated parameters convergence with respect to process noise covariance matrix, with a load torque of 12Nm.

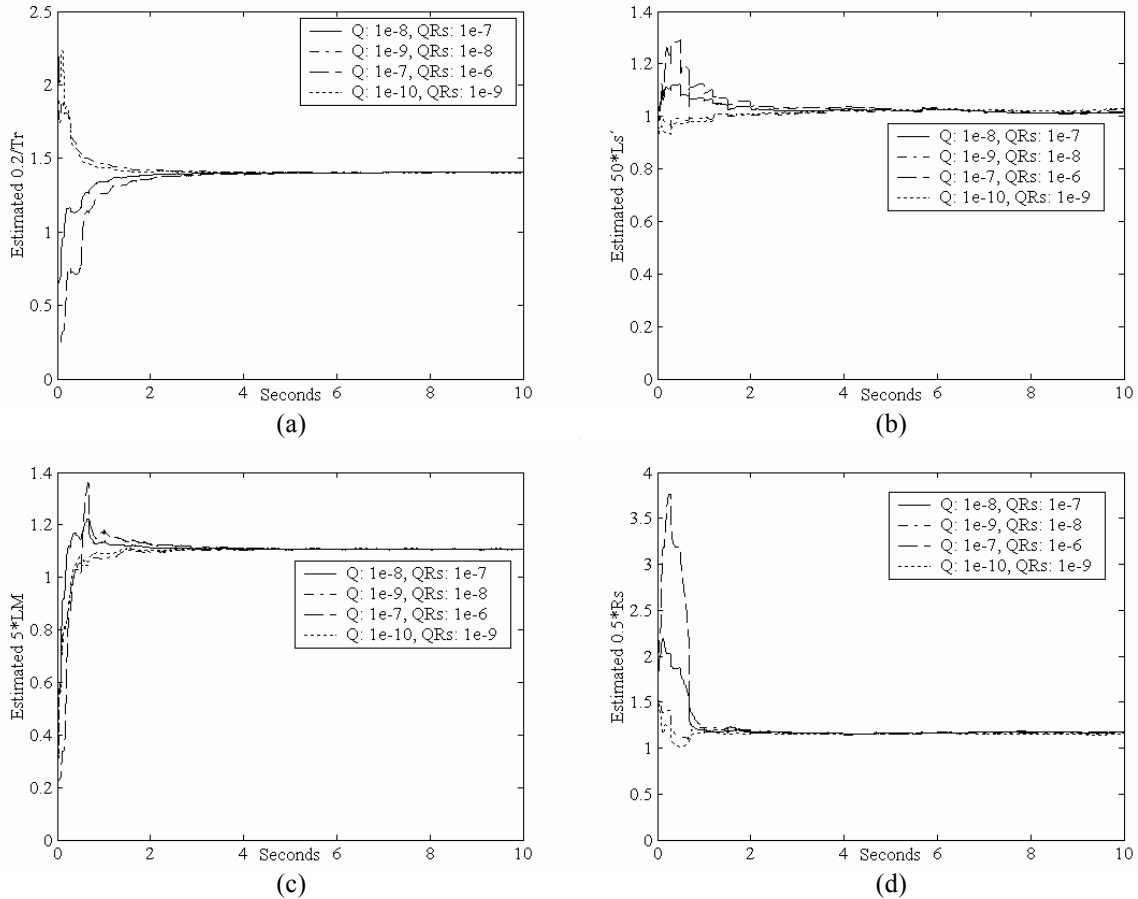


Fig. 2: Robustness test of estimated parameters convergence with respect to process noise covariance matrix (Q =diag. element of process cov. matrix), with a load torque of 12Nm. (a) estimated $0.2 \times \tau_r$, (b) estimated $50 \times L_s'$, (c) estimated $5 \times L_M$, (d) estimated $0.5 \times R_s$.

A good convergence with respect to different process covariance matrix diagonal elements can be observed. By means of the exponential functions (24) the duration of convergence phase is reduced due to the EKF dynamics improvement during the first iterations in the way to the steady state dynamics for noise rejection and parameter tracking. The robustness of the algorithm is also assured with respect to different values of measurement noise covariance R_m . Additionally, convergence speed of the states can be tuned by this parameter of the algorithm.

Simulation tests showed that the proposed algorithm works very well with different load conditions as we can see in figure 3 where estimated parameters with a load torque of 12Nm and no load and including start-up transient, are presented. The difference between start-up transient inclusion or not has no important differences in the estimated parameters final values, as can be seen in figure 4, and only affect the time and the form of the parameters convergence, namely stator resistance. This is true provided that at the time of estimation start the same dynamic conditions are warranted. It is in this situation that the filter should be particularly dynamic relatively to stator resistance. This justifies the difference between $g_{1,2,3}$ and g_4 in (24).

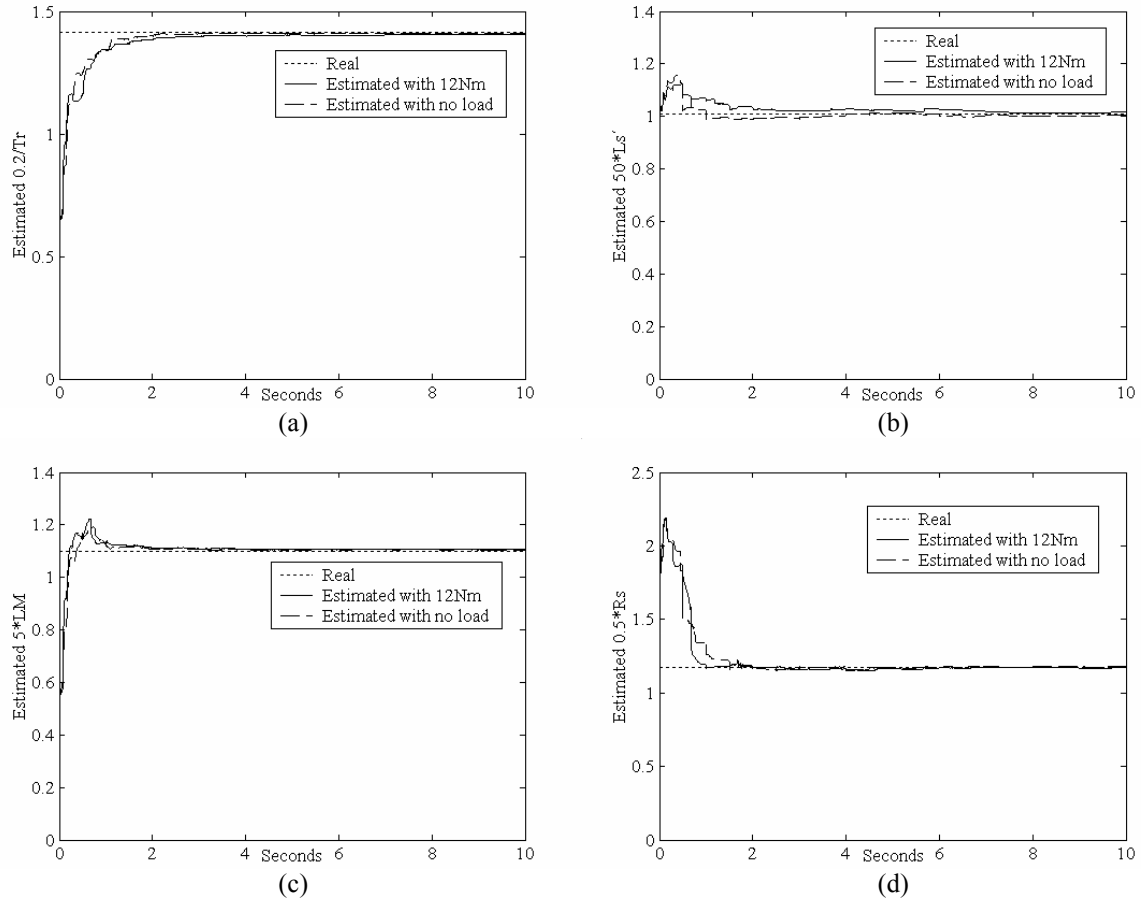


Fig. 3: Estimated parameters with a load torque of 12Nm and no load, including start-up transient. (a) estimated $0.2 \times \tau_r$, (b) estimated $50 \times L_s'$, (c) estimated $5 \times L_M$, (d) estimated $0.5 \times R_S$.

Table I show the estimated parameters values, obtained by the simulation tests presented above. It can be seen that the induction motor parameters are precisely estimated when compared with the ones obtained by classical methods and used in the simulation tests.

Table I: Estimated parameters values, obtained by simulation tests.

	By classical methods	Including start-up transient		Without start-up transient	
		With 12Nm test	With no load	With 12Nm test	With no load
τ_r (ms)	141.4	142.2	141.7	141.9	142.4
L_S' (mH)	20.2	20.3	20.1	20.1	20.4
L_M (mH)	220.1	221.1	221.0	221.1	221.3
R_S (Ω)	2.34	2.3419	2.3547	2.363	2.3382

After the state estimate values are properly stabilized the dynamic conditions can be removed and the dynamics of EKF should become less sensitive to new measurements, but sensitive enough to track parameters variations which is very slow for the stator resistance, since it varies with temperature. Rotor parameters do not need these requirements being precisely estimated with a good performance convergence.

The same global results can also be obtained with a square wave speed reference component with magnitude as low as 200 rpm, in the range of 1300 to 1500 rpm or 200 to 400 rpm.

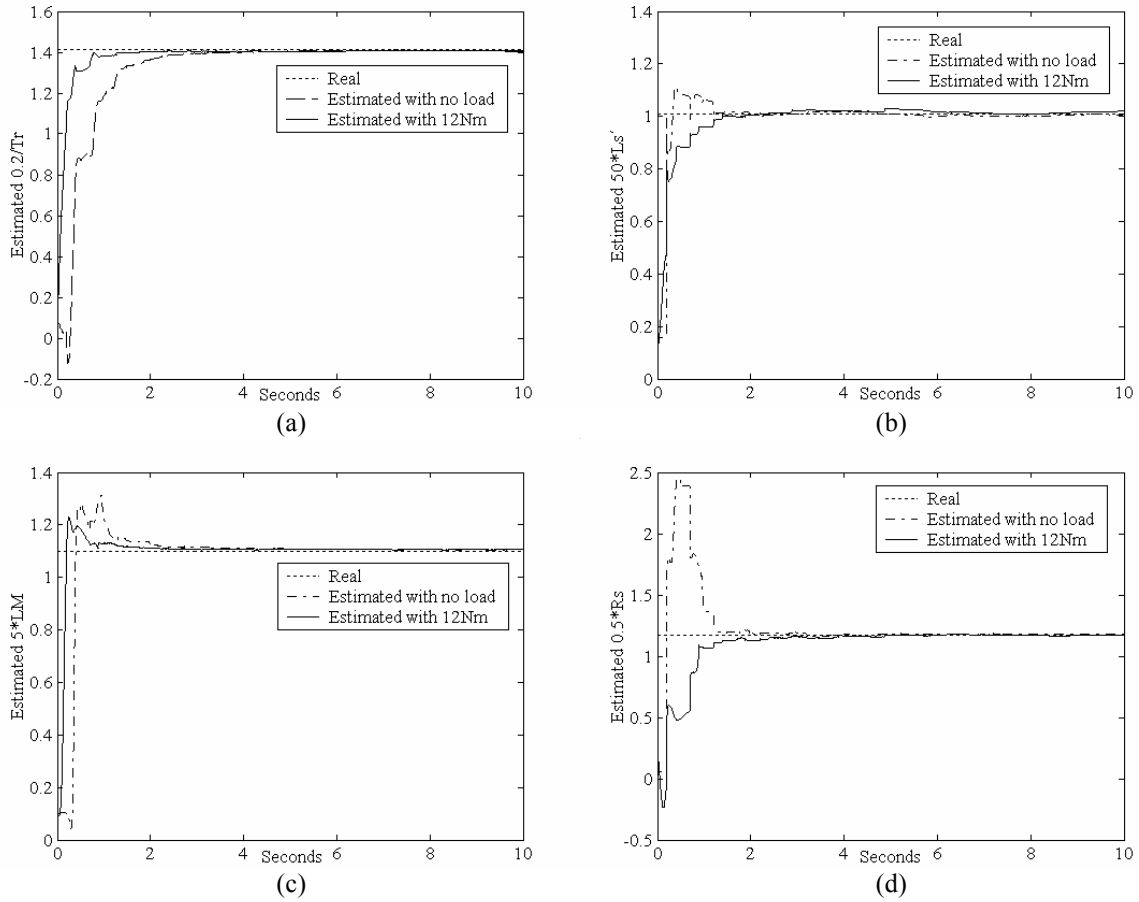


Fig. 4: Estimated parameters with a load torque of 12Nm and no load, without start-up transient. (a) estimated $0.2 \times \tau_r$, (b) estimated $50 \times L_s'$, (c) estimated $5 \times L_M$, (d) estimated $0.5 \times R_s$.

Experimental Results

For simulation and experimental purposes a 3kW squirrel-cage induction motor was used (rated voltage 400V, current 6.3A, speed 1430 rpm, frequency 50Hz, 2 pole pairs). The following set of electrical parameters was obtained by classical methods: stator resistance 2.34Ω (DC test with the induction motor at ambient temperature), rotor resistance 1.7Ω , stator and rotor inductances 240.3mH and magnetising inductance 230mH. The load torque is programmable by the module MODMEC3 from *Leroy Somer* that controls a powder brake. The voltage, current and speed signals are available in the range of $\pm 10V$ in both rotor and stator reference frames by using the AD2S100 analogue vector processor. The hardware [13] has an adjustable cutoff frequency with an accurate analogue elliptic low-pass filter, with *MAX7411*, to avoid aliasing errors. Data was collected at a sampling rate of 2.5kHz by using a 16 bits *PCI-6035E* data acquisition card and a *SC-2040* module with 8 SSH channels for simultaneous acquisition, both from *National Instruments*. The EKF algorithms were developed in *MATLAB* language and calculations were made off-line. The induction machine is controlled by an industrial frequency converter *ACS-601-0006-3* from *ABB* and the vector control scheme developed in *MATLAB* and the one implemented by *ABB* are not the same. Therefore some differences exist with respect to the evolution of the estimated parameters in the two phases of the work.

The considerations of EKF algorithms initialization presented in the preceding section should be also applicable here. The identification test consists of a start-up followed by a serial of commutations in speed reference between 200 and 1500rpm with a load torque of 12Nm, that is to say, about half of its rated value. Figure 5, from (b) to (e), shows, in solid lines, the estimated states convergence with a

load torque of 12Nm. Figure 5 (a) shows the measured electrical speed of the induction motor controlled by the *ACS-601* frequency converter. Figure 5 (f) shows estimated flux *dq* components. Also presented in figure 5 (b) to (e) with a dotted line is the evolution of the estimated parameters, if the exponential functions (24) were not used. With experimental data its functionality is yet more important to raise the speed of convergence of the state estimates, when the algorithm starts, by improving the filter dynamics by means of high values of the process noise covariance matrix diagonal elements. These values decrease exponentially with time to the steady state values to guarantee filter stability and parameters tracking. Another reason to improve the dynamics at the beginning is that measured signals are much more close to sinusoidal form than those from simulation. As a consequence the time convergence of the algorithm rises as can be seen in figure 5.

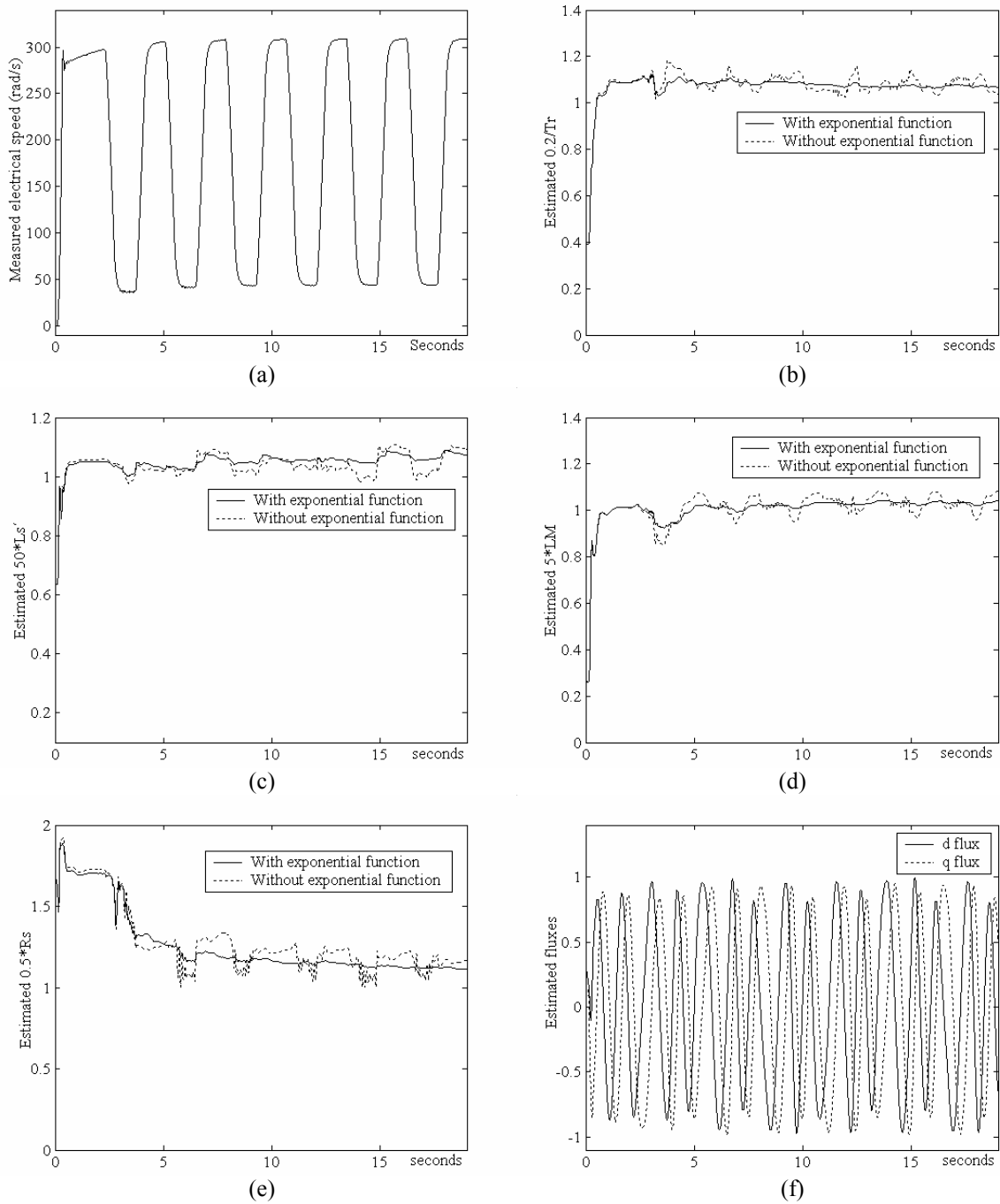


Fig. 5: Estimated states convergence with a load torque of 12Nm. (a) Measured electrical speed, (b) estimated $0.2 \times \tau_r$, (c) estimated $50 \times L_s'$, (d) estimated $5 \times L_M$, (e) estimated $0.5 \times R_s$, (f) estimated *dq* flux components.

In both simulation and experimental tests the 1st and 2nd orders of the equations (7) was used for the discretization of state equation (8) and the results showed that the 1st order proves to be sufficient, provided that the derivative of the stator current signal is computed as in output equation (11).

Table II show the estimated parameters values, obtained by experimental tests. Additional tests permitted to conclude that the estimation can be performed at lower sampling rates with the same convergence characteristics and the results to the sampling frequency of 1kHz are presented in last column of table II.

Table II: Estimated parameters values, obtained by experimental tests.

	By classical methods	Including start-up transient and 12Nm	Without start-up transient and 12Nm	Including start-up transient, 12Nm load and $f_s=1\text{kHz}$
τ_r (ms)	141.4	188.5	182.9	188.0
L_S' (mH)	20.2	22.0	19.4	22.7
L_M (mH)	220.1	208.3	206.3	205.0
R_S (Ω)	2.34	2.2146	2.2191	2.2302

To conclude the identification procedure it is necessary to validate the identified model through some validation test to evaluate the performance of the EKF algorithm. The validation test was based on the simulation of a modified induction motor model, with the estimated parameters, by injection of the measured voltages and angular velocity and subsequent comparison of simulated and measured stator current dq components.

The results are shown in figure 6 (a), for the estimated parameters and in figure 6 (b) for the parameters estimated by classical methods. As can be seen the simulated and experimental currents are very similar in the first case. So the EKF algorithm for full, parameters and fluxes, estimation is capable of fitting adequately this input-output data set with this identified model.

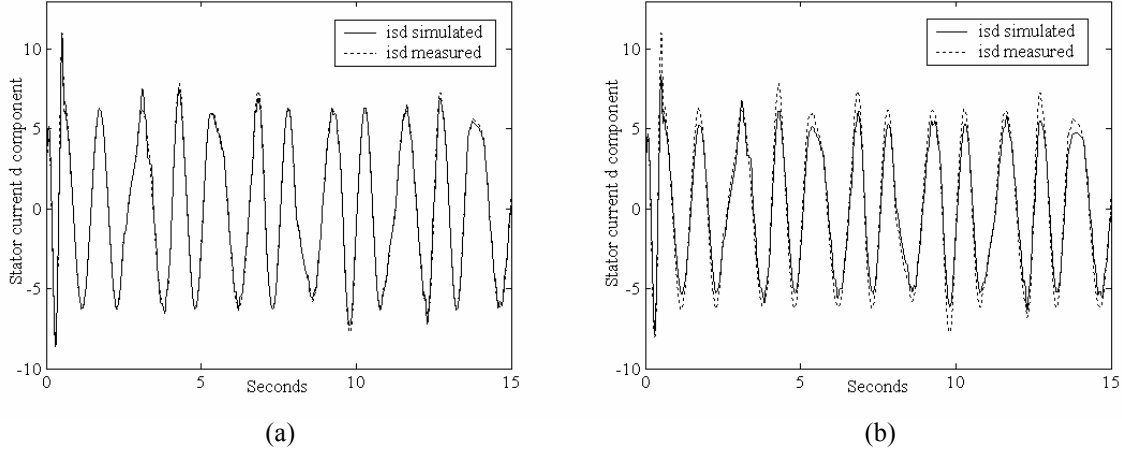


Fig. 6: Measured and simulated stator current d component. (a) Simulated current with estimated parameters by EKF, and (b) with parameters estimated by classical methods.

Conclusions

A new approach is proposed in this paper for discretization of the induction motor model to obtain a reduced order model with four electrical parameters and a single (scalar) output equation. The robustness of the algorithm initialization and convergence is presented. A series of initial square pulses in the motor speed reference is suggested to improve the speed of convergence and asymptotic behavior of the stator parameters, mainly for stator resistance estimation.

Due to the different magnitudes of the original states in the state vector these were scaled to avoid numerical problems and carry out correct estimations.

A diagonal process noise covariance matrix, weighted by exponential functions, was used to increase the speed of convergence of the state estimates when the algorithm starts, improving the filter dynamics by means of high values of the covariance matrix diagonal elements. These values decrease exponentially with time to the steady state values to guarantee filter stability and parameter tracking.

The rotor reference frame is very useful since the signals' frequency ranges are lower than in the stator reference frame and consequently, the sampling period can be made longer as well as computation cadency. The sampling frequency can be as low as 1 kHz while in the stator reference frame is usually in the range of 5 to 10kHz. This, together with the reduced order model, allows cutting down on the computational effort, which is one main drawback of the EKF. The algorithm described in this paper was tested off-line but can be implemented and is prepared for on-line estimation of all the physical induction motor parameters and is not restricted to steady state operation being capable to operate in transient conditions. Moreover, as the EKF can deal with time-varying linear plant model structures, the rotor flux and the parameters can be estimated while the rotor speed is varying such as proposed. Therefore, this approach is useful for auto-tuning and adaptive direct field-oriented induction motor control.

Simulation and experimental studies presented in this paper highlight the improvements of this new approach based on an extended Kalman filtering technique under real operation conditions.

References

- [1] Krishnan R., Bharadwaj A. S.: *A Review of Parameter Sensitivity and Adaptation in Indirect Vector Controlled Induction Motor Drive Systems*, IEEE Trans. on Power Electr., vol. 6, October 1991, n.º 4, pp. 695-703.
- [2] Finch J. W., Atkinson D. J., Acarnley P. P.: *Full-Order Estimator for Induction Motor States and Parameters*, IEE Electr. Power Appl., May 1998, vol. 145, n.º 3, pp. 169-179.
- [3] Loron L., Laliberté G., *Application of the Extended Kalman Filter to Parameters Estimation of Induction Motors*, in Proc. EPE, Brighton, 1993 pp. 85-90.
- [4] Lin F.-J.: *Robust Speed-Controlled Induction-Motor Drive Using EKF and RLS Estimators*, IEE Proc.-Electr. Power Appl., vol. 143, May 1996, n.º 3, pp. 186-192.
- [5] Atkinson D. J., Acarnley P. P., Finch J. W.: *Observers for Induction Motor State and Parameter Estimation*, IEEE Transactions on Industry Appl., vol. 27, November/December 1991, n.º 6, pp. 1119-1127.
- [6] Aquilla A. D., Cupertino F., Salvatore L., Stasi S.: *Kalman Filter Estimators Applied to Robust Control of Induction Motor Drives*, IECON'98, Aachen, Germany, 1998, pp. 2257-2262.
- [7] Wade S., Dunnigan M. W., Williams B. W.: *Modeling and Simulation of Induction Machine Vector Control with Rotor Resistance Identification*, IEEE Trans. on Power Electr., vol. 12, May 1997, n.º 3, pp. 495-506.
- [8] Aquilla A. D., Papa S., Salvatore L., Stasi S.: *A Delayed Kalman Filter for On-Line Estimation of Induction Motor Parameters and Rotor Flux Space Vector Position*, MELECON'96, pp. 269-273.
- [9] Aksoy S., Altas I. H., Eker M. K.: *A Reduced Order Rotor Time Constant and Flux Estimator for Vector Controlled Induction Motor*, MELECON'96, pp. 274-277.
- [10] Walker É., Pronzato L.: *Identification of Parametric Models from Experimental Data*, Masson, 1997.
- [11] Vas P.: *Parameter Estimation, Condition Monitoring, and Diagnosis of Electrical Machines*, Oxford Science Publications, 1993.
- [12] Astrom, K. J., Wittenmark, B.: *Computer Controlled Systems: Theory and Design*, Prentice-Hall, 1997.
- [13] Leite V., Teixeira H., Araújo R., Freitas D.: *Sistema Eletrónico de Condicionamento e Processamento, em Tempo Real, das Tensões e Correntes do Motor de Indução Trifásico Alimentado por Conversores de Frequência*, 7^{as} Jornadas Hispano-Lusas de Ingeniería Eléctrica, Madrid, Spain, July, 2001, vol. IV